Hydrostatic driving system for self-propelled sprayer

Zou Fan[1], Kang Jingjing[1], Xiao Maohua[1*], Song Xucheng[1], Ji Guojun[2]

(1. *College of Engineering, Nanjing Agricultural University, Nanjing 210031, China*;
2. *Essen Agricultural Machinery Changzhou Co., Ltd., Changzhou 213200, China*)

Abstract: The aim of this paper is to design a transmission system based on HST hydraulic drive technology, which was designed for the traditional self-propelled sprayer when mechanical transmission is large, and it is prone to subsidence and slipping in the field, especially in paddy field. Firstly, the overall transmission scheme was designed on the basis of the overall layout in the medicine box, and the technical parameters were determined according to the working conditions and load analysis. Secondly, the simulation model of the self-propelled sprayer was constructed by AMESim software. Finally, according to the simulation results and the design of the program, the walking performance experiment was carried out on the experimental model of Essen. The experiment was carried out on the performance test of the HST and the speed control analysis. The stable output flow of the main pump is 78.8 L/min, the load stable speed and the load torque are 33.2 r/min, 772.6 N·m, respectively, compared with the traditional mechanical transmission. Left and right roll angles and front and rear pitch angles fluctuation ranges are small. The simulation and prototype experiments showed that the designed transmission system was stable and responsive, and it could meet the requirement of effectively reducing the weight.

Keywords: self-propelled sprayer, HST, transmission system, hydraulic drive, AMESim

Citation: Zou, F., J. J. Kang, M. H. Xiao, X. C. Song, and G. J. Ji. 2017. Hydrostatic driving system for self-propelled sprayer. International Agricultural Engineering Journal, 26(3): 12–18.

1 Introduction

Food is the first necessity of the people, and the high yield of major crops such as rice, soybeans and corn is very important to the livelihood of the people, thus controlling pests and diseases for crops is especially important. At present, the agricultural pest control is mainly used traction sprayers in China, the chassis from the ground to a small gap and high weight makes it difficult to spray on the growth of rice and other tall crops. However, the cultivation of rice in China is mostly located in the south, the soil has complex rheological and thixotropic characteristics. The operating conditions are more complex, and the large and medium-sized plant protection machinery is not suitable for a long time (Gu et al., 2000). Therefore, in order to improve the mechanization level of rice plant protection in China, it is of great significance to develop plant protection machinery driving system which adapts to various working conditions.

Hydrostatic Static Transmission (HST) is widely used in agricultural machinery because of its small size, light weight and easy operation (Gao et al., 2017), such as John Deere's 4730 sprayer (Zaman et al., 2011). HST technology has been applied to tractors (Batte et al., 2006) and combine harvesters in China (Sun et al., 2014), But compared with other countries, in China, there is a big gap among the same type of hydrostatic CVT transmission in quality (Zhang, 2014; Liu et al., 2016).

Compared with the traditional mechanical transmission, the driving mode of hydraulic full drive based on HST has the advantages of small quality when no-load, stable transmission performance, easy maintenance and other advantages (Huang and Su, 2010), can greatly reduce the quality of the spray machine, improve the sprayer in the field especially when the performance of the paddy field walking (Wang et al.,

Received date: 2017-05-31 **Accepted date:** 2017-08-02

* **Corresponding author: Xiao Maohua**, Associate Professor, Doctor. Department of Mechanical Engineering, Nanjing Agricultural University, Nanjing 210031, China. Email: zoufan1997@163.com.

2014). Therefore, a transmission scheme based on HST technology with small quality and stable transmission performance was designed in this paper. Simulation analysis and experimental verification were also carried out.

2 Layout of the machine and technical requirements

2.1 Layout of the machine

In this paper, the program was arranged in the medicine box whose gravity was always more stable. The layout of each part of the machine is shown in Figure 1.

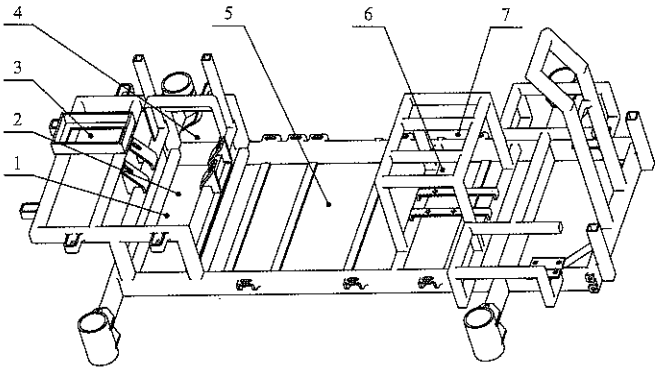

1. Driven hydraulic pump 2. Diesel tank 3. Hydraulic oil tank 4. Diesel engine 5. Medicine chest 6. Application of hydraulic pump 7. Chair

Figure 1 Layout scheme of the sprayer

The hydraulic layout scheme enabled the sprayer to operate smoothly in the complicated and changeable road conditions, and effectively reduced the risk of accidents such as rollover (Du et al., 2014).

2.2 Technical requirements

According to the characteristics of field operations (Ji et al., 1999) and the actual performance requirements of the sprayer, the main technical parameters required by the sprayer designed were shown in Table 1.

Table 1 Main technical parameters of sprayer

Project	Unit	Technical parameter
Machine quality	kg	900
Working pressure	MPa	0.4-1.0
Maximum spray amplitude	m	12
Ground clearance	mm	1100
Theoretical operation speed	Km h^{-1}	1-5
Barrel capacity	L	500
Maximum gradient	°	20

Considering the fact that the sprayer was mainly used in the field and on the road, the road condition was relatively simple, but the road conditions in the field were more complicated, so the horizontal bending condition, torsion, emergency braking and emergency turning condition, the four common conditions were mainly considered.

3 Analysis and design of Hydraulic Driving System of the sprayer

3.1 Load analysis of Hydraulic Driving? System

When climbing: $M_t=M+M_f+M_a$

When activated: $M_t=M+M_f+M_a$

Stable operation: $M_t=M+M_f$

When deceleration was stopped:

$$M_t=M+M_f-M_a \quad (1)$$

The M_t in the formula was the total load that the motor overcame, N·m; M was the working load torque, N·m; M_f was the torque of the rotating part to the motor shaft diameter, N·m; M_a was the inertia moment of the hydraulic pressure in the wheel and the motor at start and stop, N·m.

The maximum traction during travel was about:

$$F_t = G\cdot\sin\alpha + G\cdot f\cdot\cos\alpha \quad (2)$$

The maximum torque was:

$$M_z=F_t\cdot R/\eta X \quad (3)$$

where, ηX was the mechanical efficiency of the sprayer.

According to the calculated load value and the size of the motor, the working pressure of the hydraulic system was selected, and the economic factor and the specifications of the existing hydraulic component were taken into account (Zhi et al., 2010). By the maximum traction force of 5718.34 N, can be the primary working pressure of 19 MPa.

3.2 Design scheme of Hydraulic Driving System

Compared with the open system, closed system, although the structure is complex, needs to be designed a separate cooling device, while the fuel tank has small size, compact structure, the oil is not easy to be contaminated and stable performance, suitable for volume control circuit. Therefore, closed hydraulic circuit was used.

The hydraulic system used twin pumps, the main pump was an inclined plate axial plunger variable pump, and the auxiliary pump was one-way quantitative hydraulic pump. At the same time, a closed loop was formed by four variable motors.The speed change device

was manual servo valve. The overall scheme of the hydraulic driving system was shown in Figure 2.Among them, Changchai 3M78 diesel engine was chosen for this experiment as it uses the tunnel structure, the vibration is small, and the noise is low. The oil of the feeding, steering and servo control circuit was supplied by the auxiliary pump of the system through the priority valve, that is, the hydraulic power was provided by the auxiliary pump through the priority valve to the charge system, steering system, servo control system to provide hydraulic power. When there is no steering nor speed change, the auxiliary pump enters the priority valve through the oil inlet P, and then enters the oil supplying circuit from the oil outlet EF. When the turn occurred, the priority valve supplied hydraulic oil from the DF port to the steering loop first, and the steering loop hydraulic oil directly got into the oil supply loop to achieve oil supplying function. When the speed need to be changed, the auxiliary pump provided pressure oil to the manual servo valve 3, and then entered the pump servo hydraulic cylinder to control swashplate swinging, regulate pump or motor displacement, so as to achieve the sprayer drive at different speeds.

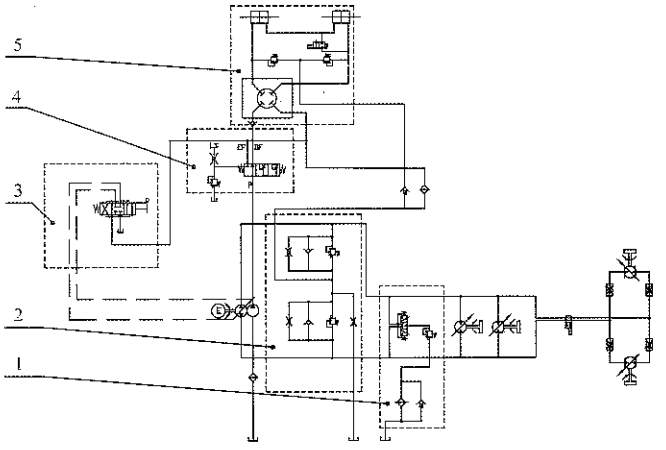

1. Cooling circuit 2. Fill oil circuit 3. Manual servo valve 4. Priority valve 5. Turn circuit

Figure 2 Schematic diagram of hydraulic system

As the pump and motor were integrated with a variety of valves, the structure was compact, easy to be arranged. Because of the closed circuit, the fuel tank was small in size, and the whole seal of the tank could reduce pollution. The variable pump and variable motor can be adjusted conveniently. Only one Joystick can realize forward, backward and stepless speed was changed. The closed loop system composed of pump and motor can also realize bidirectional reversible transmission. The four wheel synchronous drive was realized by the motor parallel loop, and the aim of locking the rear wheel, the four wheel steering and the two wheel steering switching were realized, and the walking performance of the sprayer was improved.

4 Modeling, simulation and verification on AMESim

4.1 Build simulation model

Based on the above design and analysis, the simulation model of the hydraulic transmission of the sprayer was built in the AMEsim software, as shown in Figure 3, the main simulation parameters were shown in Table 2.

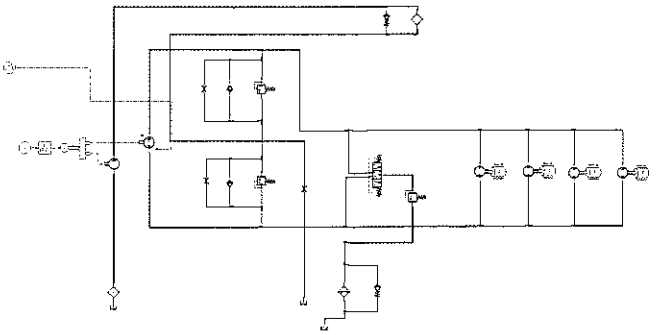

Figure 3 Simulation model of hydraulic transmission of sprayer

Table 2 Simulation parameters

Parameter	Unit	Value
Engine speed	r/min	3600
Displacement of hydraulic main pump	mL/r	21.8
Displacement of charge pump	mL/r	4.1
Motor displacement	Ml/r	380
Motor maximum speed	r/min	800
Load moment of inertia	kg m^2	35.34
Load torque	N·m	739.44
Safety valve	MPa	25

Since there was no twin pumps model in hydraulic press, the main pump and the auxiliary pump were separated and connected to the engine respectively. The signal source sent a constant signal, which was converted to the speed output of the engine through a signal converter, and then it was connected to the speed input end of the two pumps. The equivalent rotation inertia, sliding friction and static friction can be set up by using load rotating dynamics model instead of wheel. The manual servo valve was replaced with a signal source

to control the displacement of the variable pump or motor and the speed of the sprayer (Xin et al., 2010).

4.2 Simulation analysis

4.2.1 HST performance test simulation

The preferred sub model was assigned to each component, and the component parameters were entered according to Table 2, the simulation time was set to 15 s and the step was 0.01 (Yuan et al., 2013).

After the simulation is completed, the flow of the two-way hydraulic main pump and auxiliary pump, hydraulic motor flow and pressure, the speed and torque curve of the load were shown as the follows (Figures 4, 5, and 6).

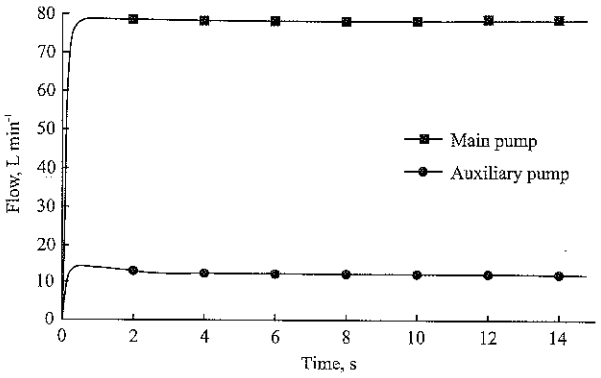

Figure 4 Flow rate of two-way hydraulic main pump and auxiliary pump

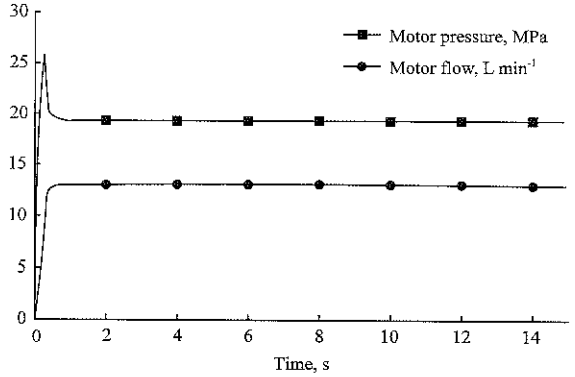

Figure 5 Motor flow and pressure curve

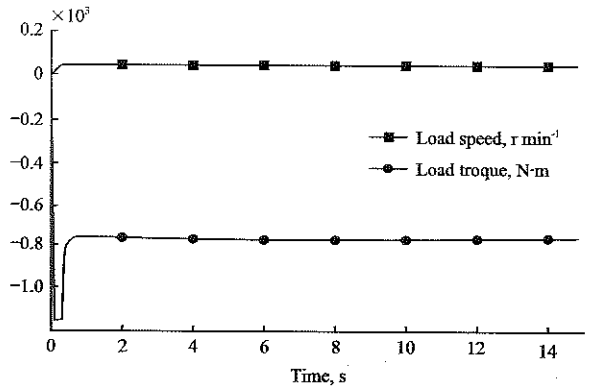

Figure 6 Speed and torque curve of load

As can be seen from Figure 4, the steady output flow of the hydraulic main pump was 78.8 r/min, which was slightly larger than the maximum output flow of the PY-21.8 hydraulic pump. However, considering the simulation of the hydraulic pump, the existence of hydraulic oil leaks was neglected. The result of simulation was in the error range. According to Figure 5 and Figure 6, the steady output flow and the pressure of the motor were within the normal range of operation. It can be seen from Figure 6 that the load stable speed and load torque were 33.2 r/min and 772.6 N·m respectively, and the speed of the load (motor speed) should be greater than 30.8 r/s when the sprayer was running at the fastest speed of 5 km/h, simultaneously, the load torque (motor torque) should be greater than 739.4 N·m, so the simulation results met the design requirements (Zhang et al., 2010).

4.2.2 Speed analysis

As mentioned above, the system changed the angle of the swashplate of the pump by manual servo valve to change the displacement of the hydraulic pump so as to achieve the purpose of speed regulation. As the AMESim hydraulic library did not have a manual servo valve model, the output parameters of the variable pump were changed by using the signal source to change the displacement of the main pump.

The main input parameters of the main pump are shown in Table 3.

Table 3 Variable pump control parameters

Initial value	Terminal value	Run time, s	Stage
0	+1	5	Accelerated start
+1	+1	10	Positive uniform
+1	−1	10	From positive to reverse
−1	−1	10	Reverse uniform
−1	+1	10	From reverse to positive

The simulation time was set to 60 s and the step was 0.01. Click the start, after the simulation was completed, we can get the main pump variable coefficient changes, hydraulic motor and flow, load speed, load torque curve, which were as the follows (Figures 7 to 10).

As can be seen from Figure 8, the flow and pressure of the motor were basically stable at all stages of the speed and coincide with the trend of the speed. When the displacement was close to zero, the motor flow and speed

were zero at a certain stage, which was also consistent with that the motor had critical speed characteristics consistent. In contrast to Figures 7, 9 and 10, the change of load speed and torque was consistent with the change of the main pump displacement to achieve the speed change, and the change was relatively stable. Therefore, the results can be seen that the performance of hydraulic transmission system is relatively stable and can adapt to the sprayer speed requirements.

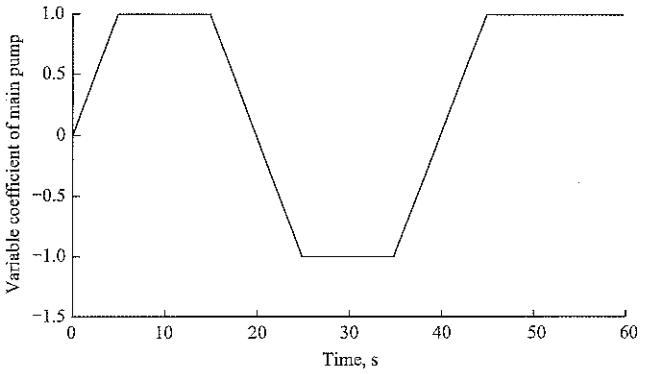

Figure 7 Variable coefficient curve of the main pump

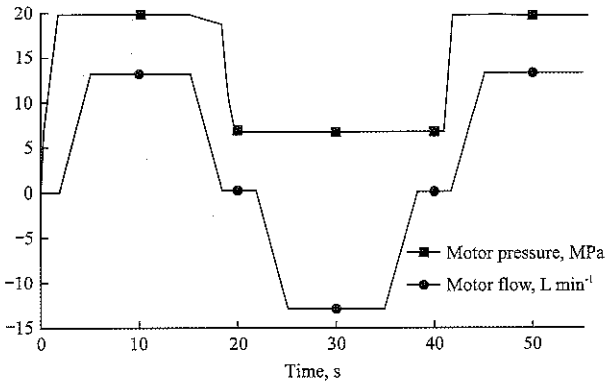

Figure 8 Motor flow and pressure curves

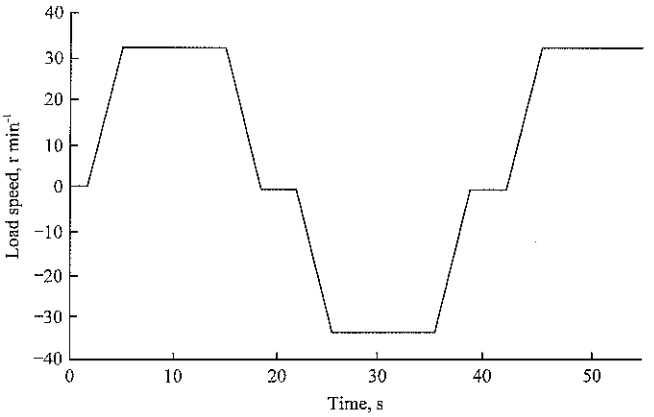

Figure 9 Load speed curve

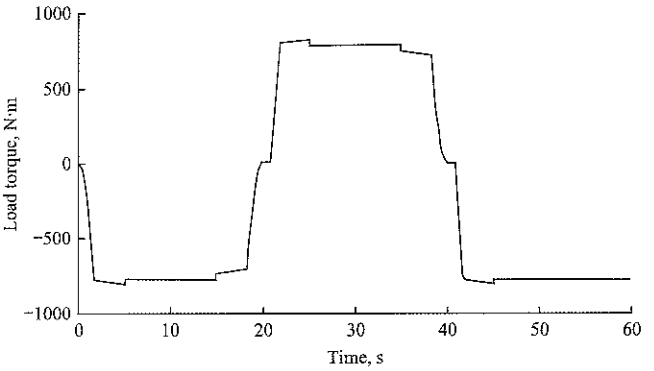

Figure 10 Load torque curve

5 Test verification

After the hydraulic system design was completed, the test prototype was produced in cooperation with Essen Agricultural Machinery Co., Ltd. The hydraulic system designed in the previous design was carried out on the test prototype of the Essen agricultural machine. Test prototype and test ramp were shown in Figure 11.

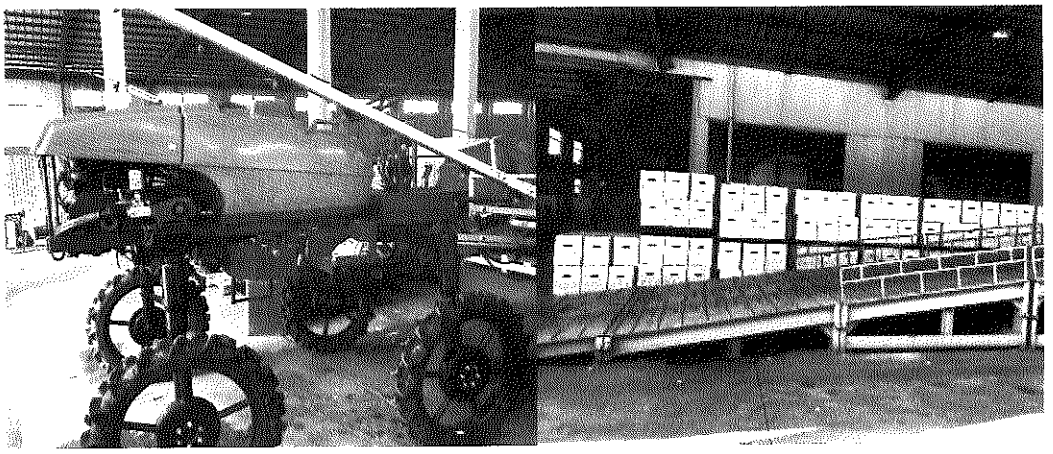

Figure 11 Test prototype and test ramp

Two typical working conditions, the running test of the rugged field work and the upper and lower ramp were tested. The dynamic monitoring data of two indexes, left and right roll angle and front and rear pitch angle, are mainly monitored to characterize the stability of the system and to test ride comfort. (The test instrument was

mounted in the middle of the machine).

Angle sensor real-time detection data analysis, and processing results were shown in Figure 12. When driving in rugged fields, the pitch angle fluctuates in the range of 10°, and the fluctuation range of the obstacle is 20° due to the large fluctuation of the road or the gravel. The whole sprayer is stable and reliable. The test ramp is about 20 degrees, and the surface of the ramp has certain fluctuations whose ups and downs are in the range of about 5 degrees. The design meets the requirements, which can adapt the needs of a variety of operating conditions.

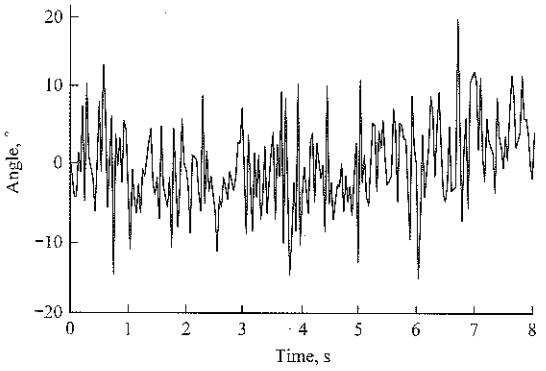

a. Rugged road front and rear pitch angle

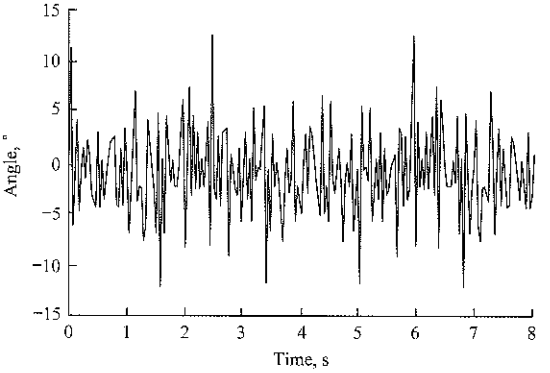

b. Rugged road around the roll angle

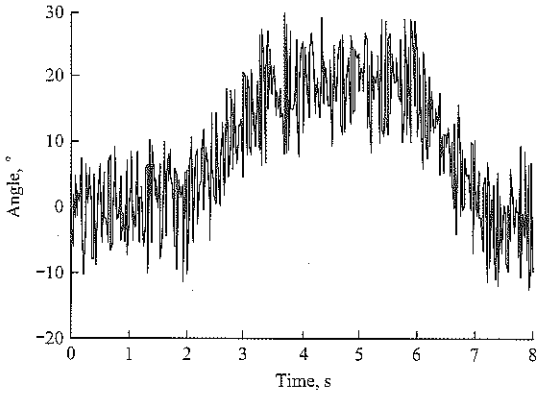

c. Uphill before and after the pitch angle

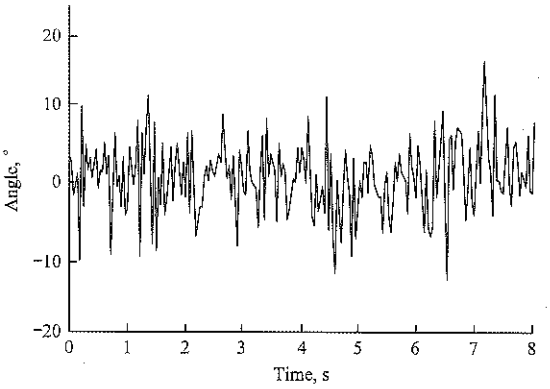

d. Uphill left and right roll angle

Figure 12 Rugged terrain and hillside test results

6 Conclusions

(1) Based on HST full hydraulic drive, the transmission system was designed for the self-propelled sprayer, and the functions of steering, speed and cooling were realized.

(2) Through building the mode and analyzing it in the AMEsim software, the simulation test and prototype test results showed that the design of hydraulic program was accurate, fast, stable, and met the operational requirements.

(3) The research will be helpful to optimize the hydraulic transmission system of the paddy field sprayer and reduce the weight of water field spray machine, which is of reference value for the application of agricultural plant protection machinery and HST technology in agriculture.

Acknowledgments

The research is funded partially by Central University of Basic Scientific Research Business Special Funds (KYZ201760), Jiangsu Province, Six Talent Summit Project (2015-ZBZZ-011) and Nanjing Agricultural University College of Technology Outstanding Young Talent Science and Technology Fund (YQ201605) and Nanjing Agricultural University Students Innovation Training (1630B16).

[References]

[1] Batte, M. T., and M. R. Ehsani. 2006. The economics of precision guidance with auto-boom control for farmer-owned agricultural sprayers. *Computers & Electronics in Agriculture*, 53(1): 28–44.

[2] Du, J., G. Zhang, T. Liu, and S. To. 2014. Improvement on

load performance of externally pressurized gas journal bearings by opening pressure-equalizing grooves. *Tribology International,* 73(5): 156–166.

[3] Gao, X., J. Guo, Z.Zhu, and S. Han. 2017. Design of Power Transmission System of High-clearance Self-propelled Sprayer. *Journal of Agricultural Mechanization Research,* 39(4): 247–268.

[4] Gu, D. X., G.R.Zhang, R. J. Zhang, and Y. Peng. 2000. Review on fifty-years biological control of insect pests in southern China. *Acta Entomologica Sinica*, 43(3): 327–335.

[5] Huang, K. J., and H. W. Su. 2010. Approaches to parametric element constructions and dynamic analyses of spur/helical gears including modifications and undercutting. *Finite Elements in Analysis & Design,* 46(12): 1106–1113.

[6] Ji, C. Y., Z. X. Lu, and J. Z. Pan. 1999. Analysis of bearing capacity and adhesion to solid surfaces of paddy soils. *Journal of Nanjing Agricultural University,* 22(4): 105–108. (In Chinese with English abstract)

[7] Liu, X. M., Y. Li, M. Li, J. Yuan, and Q. Fang. 2016. Design and Test of Smart-targeting Spraying System on Boom Sprayer. *Transactions of the Chinese Society for Agricultural Machinery*, 47(3): 37–44. (In Chinese with English abstract)

[8] Sun, S. M., J. G. Wang, and K. E. Jian. 2014. New HST optimal design and test in harvester. *Journal of Machine Design*, 2014(5): 34–38.

[9] Wang, X. N., X. K. He, A. Herbst, L. Jan, and J. Zheng. 2014. Development and performance test of spray drift test system for sprayer with bar. *Transactions of the Chinese Society of Agricultural Engineering*, 30(18): 55–62. (In Chinese with English abstract)

[10] Xin, F. U., M. Xu, and W. Wang. 2010. Hydraulic system design and simulation of the forging manipulator. *Journal of Mechanical Engineering*, 46(11): 49–54.

[11] Yuan, S. H., C. B.Yin, and S. H. Liu. 2013. Working properties of counterbalance valve based on AMESim Code. *Transactions of the Chinese Society for Agricultural Machinery*, 44(8): 273–280. (In Chinese with English abstract)

[12] Zaman, Q. U., T. J. Esau, A. W. Schumann, D. C. Percival, and Y. K. Chang. 2011. Original papers: Development of prototype automated variable rate sprayer for real-time spot-application of agrochemicals in wild blueberry fields. *Computers & Electronics in Agriculture*, 76(2): 175–182.

[13] Zhang, L. J. 2014. Design and performance analysis of Self-propelled Boom Sprayer. M.S. thesis, Jiangsu University.

[14] Zhang, T. T., M. Chen, and H. M. Chen. 2010. The designing and optimizing of fully hydraulic driving system of engineering machinery based on Matlab. *Journal of Machine Design*, 27(3): 58–61.

[15] Zhi, Y. H., X. P. Shi, Y. S. Liu, and Z. F. Yue. 2010. Dynamical optimization design on pipe diameter and pipeline support of the hydraulic pressured/fuel oil pipeline system. *Journal of Machine Design*, 27(3): 75–79.